BIOCHEMISTRY
including biophysical chemistry & molecular biology
Article

Biochemistry **2009,** *48,* 5405–5416 5405
DOI: 10.1021/bi900243f

Understanding of the Binding Interface between PsaC and the PsaA/PsaB Heterodimer in Photosystem I†

Bharat Jagannathan‡ and John H. Golbeck*,‡,§

‡*Department of Biochemistry and Molecular Biology and* §*Department of Chemistry, The Pennsylvania State University, University Park, Pennsylvania 16802*

Received February 14, 2009; Revised Manuscript Received May 7, 2009

ABSTRACT: The PsaC subunit of Photosystem I (PS I) is tightly bound to the PsaA/PsaB heterodimer via an extensive network of ionic and hydrogen bonds. To improve our understanding of the design of the PsaC−PsaA/PsaB binding interface, variants of PsaC were generated, each lacking a key binding contact with the PsaA/PsaB heterodimer. The characteristics of the reconstituted, variant PS I complexes were monitored by time-resolved optical spectroscopy, low-temperature EPR spectroscopy, and electron transfer throughput measurements. In the absence of the ionic bond forming contacts $R52_C$ or $R65_C$, a markedly slower charge recombination occurs between P_{700}^+ and $[F_A/F_B]^-$. The addition of PsaD leads to the restoration of native recombination kinetics in a fraction of the PS I complexes reconstituted with $R52A_C$, but not with $R65A_C$. Contrary to expectation, the absence of $Y80_C$, which forms two symmetry-breaking H-bonds with PsaB, does not significantly affect the binding of PsaC as judged by the rate of charge recombination between P_{700}^+ and $[F_A/F_B]^-$. However, the removal of the entire C-terminus results in a dramatic decrease in the rate of charge recombination. Low-temperature EPR spectra of the variant PS I complexes indicate that the magnetic environments of F_A and F_B are altered when compared to that of native PS I. The slowing of the rate of charge recombination in the variant PS I complexes could be due to an increase in the distance between F_X and F_A/F_B as the result of non-native binding or to an altered reduction potential of the iron−sulfur clusters, which would result in a different rate of thermalization up the electron acceptor chain. The most significant finding is that the variant PS I complexes support lower rates of light-induced flavodoxin reduction and that the rates deteriorate rapidly on exposure to dioxygen due to the degradation of F_A and F_B. We suggest that the extensive set of ionic bonds and H-bonds between PsaC and the PsaA/PsaB heterodimer has evolved to ensure an exceedingly tight binding interface, thereby rendering the [4Fe-4S] clusters in PsaC inaccessible to dioxygen at the onset of oxygenic photosynthesis.

Photosystem I (PS I)[1] is a membrane-bound pigment−protein complex that catalyzes light-induced electron transfer for the purpose of generating NADPH. Cyanobacterial PS I consists of a trimer, wherein each monomer consists of 12 protein subunits. Nine of the subunits (PsaA, PsaB, PsaF, PsaI, PsaJ, PsaK, PsaL, PsaM, and PsaX) are primarily α-helical and span the membrane. PsaC, PsaD, and PsaE are bound to the surface of PS I, forming a "stromal hump", which provides a docking surface for the soluble electron acceptors ferredoxin and flavodoxin (*1*, *2*).

The electron transfer chain begins at P_{700}, a special pair of chlorophyll *a* (Chl *a*) molecules that, according to the current paradigm, functions as the primary electron donor (however, see ref (*3*) for an alternative hypothesis). The electron transfer chain immediately bifurcates into two branches, each containing two Chl *a* molecules, A_{-1A} and A_{0A} (A_{-1B} and A_{0B}), the latter of which functions as the primary electron acceptor. The initial $P_{700}^+A_{0A}^-$ ($P_{700}^+A_{0B}^-$) charge-separated state is stabilized in time by rapid electron transfer to a phylloquinone molecule, A_{1A} (A_{1B}). The branches converge at the [4Fe-4S] cluster F_X, at which point the electrons are transferred linearly through F_A and F_B to ferredoxin or flavodoxin (*4*). The cofactors P_{700} through F_X are located on the heterodimeric core of PS I (P_{700}-F_X core), which is comprised of PsaA (83 kDa), PsaB (83 kDa), and seven smaller membrane-spanning proteins. The [4Fe-4S] clusters that serve as the terminal electron acceptors, F_A and F_B, are located on PsaC (9 kDa), which is bound on the stromal surface. PsaD (15 kDa) and PsaE (8 kDa) flank PsaC on either side on the surface of PS I.

In vitro rebinding studies (*5*−*7*) and in vivo genetic deletion studies (*8*−*10*) have shown that the membrane intrinsic P_{700}-F_X core is fully formed prior to the assembly of the stromal subunits, which dock in a well-defined order: PsaC first followed by PsaD and then PsaE. Electron paramagnetic resonance (EPR) studies indicate that F_A and F_B undergo three distinct changes in their

†Supported by grants from the National Science Foundation (MCB-0519743) and the U.S. Department of Energy (DE-FG-02-98-ER20314).

*To whom correspondence should be addressed. Telephone: (814) 865-1163. Fax: (814) 863-7024. E-mail: jhg5@psu.edu.

[1]Abbreviations: PS I, Photosystem I; Chl *a*, chlorophyll *a*; DCPIP, 2,6-dichlorophenolindophenol; EPR, electron paramagnetic resonance.

Published on Web 05/11/2009

magnetic properties during the assembly of PS I: the two [4Fe-4S] clusters appear magnetically equivalent in unbound PsaC, they become inequivalent when PsaC binds to the membrane intrinsic P_{700}-F_X core, and they gain the properties of the native PS I complex after the binding of PsaD (*7*). PsaE has no influence on the magnetic properties of F_A or F_B (*7*).

PsaC binds directly above the F_X binding site (*11*), with the F_A cluster proximal to F_X (*11*−*13*). PsaC is bound via an intricate network of ionic bonds (Figure 1A) consisting of one Lys and two Arg residues on PsaC, and four Asp residues on PsaA/PsaB, two of which are part of an extrinsic loop that also provides the Cys residues that coordinate the F_X cluster. The network of Asp-Arg/Lys ionic contacts is highly C_2-symmetric; $R52_C$ forms five ionic bonds with $D568_A$ and $D579_A$, and $K51_C$ and $R65_C$ form five ionic bonds with $D555_B$ and $D566_B$ (*14*). If PsaC were rotated (in silico) 180° about the C_2 axis of symmetry, $R52_C$ would still form five ionic bonds, but with $D555_B$ and $D566_B$, and $K51_C$ and $R65_C$ would still form five ionic bonds, but with $D568_A$ and $D579_A$ (*14*). The equal division of the 10 ionic contacts between PsaA and PsaB represents a highly symmetric and extremely tight binding surface for the PsaC protein.

PsaC also forms three H-bonds (Figure 1B) in a region of the P_{700}-F_X core distant from the ionic contacts, which break the symmetry, locking PsaC into one of the two possible orientations on the PsaA/PsaB heterodimer. These bonds are formed between $T73_C$ and $Y80_C$ on the C-terminus of PsaC and $Q678_B$, $K702_B$, and $P703_B$ on a surface-located segment of PsaB (*14*). Unlike the symmetric ionic contacts, a symmetry-related binding pocket for the C-terminus of PsaC does not exist on the comparable surface-located segment of PsaA. Thus, the three H-bonds between the C-terminus of PsaC and PsaB break the otherwise-perfect binding symmetry between PsaC and the PsaA/PsaB heterodimer.

The PsaD protein adjoins PsaC on the stromal surface and has extensive interactions with PsaC and the PsaA/PsaB heterodimer. The N-terminus of PsaD covers the surface of the binding site of the C-terminus of PsaC with PsaB, forming multiple contacts with both PsaA and PsaB (*11*, *14*). The C-terminus of PsaD wraps around the stromal-facing surface of PsaC and attaches to the stromal interface of PsaB. The so-called "C-clamp" of PsaD fixes the PsaC subunit into its final configuration and additionally serves to define the binding site for ferredoxin and flavodoxin (*2*, *15*).

The large number of contacts between PsaC and the PsaA/PsaB heterodimer ensures an exceedingly tight binding interface between the protein subunits, which is demonstrated by the high concentration of chaotropic agents required to dissociate PsaC, PsaD, and PsaE from the P_{700}-F_X core (*5*). Nevertheless, it is not entirely clear whether the presence of all of the ionic bonds and H-bonds between PsaC and the PsaA/PsaB heterodimer are necessary for efficient electron transfer from F_X to F_A/F_B or if there is redundancy in the network of contacts. Namely, what happens if one or more of the PsaC−PsaA/PsaB contacts are missing? We approached this question by generating in vitro variants of PsaC followed by reconstitution onto P_{700}-F_X cores in the absence and presence of PsaD. This two-step procedure allowed us to probe not only the issue of the symmetric ionic bonds in the vicinity of F_X and the symmetry-breaking C-terminus of PsaC but also the role of the PsaD protein in the final assembly of PS I.

In this paper, we attempt to gain a better understanding of how the absence of certain binding contacts affects the assembly of PsaC during the final stage of PS I assembly. The results of this

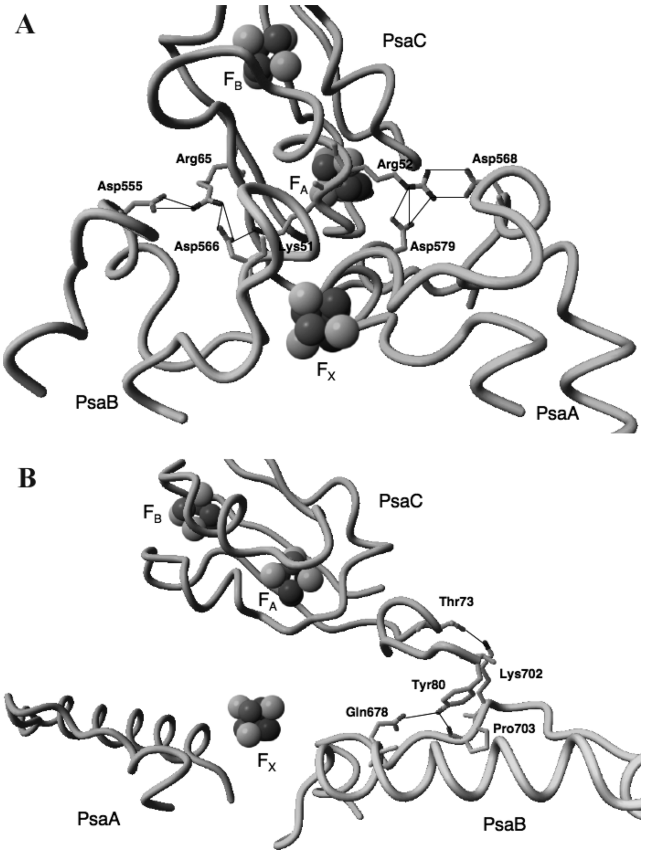

FIGURE 1: (A) Symmetric network of ionic bonds between PsaC and the PsaA/PsaB heterodimer. (B) Symmetry-breaking hydrogen bonds between PsaB and the C-terminus of PsaC (Protein Data Bank entry 1JB0).

study are discussed in the context of understanding the design philosophy of the extensive PsaC−PsaA/PsaB binding interface as a strategy for protecting the F_A and F_B clusters from oxidative denaturation at the onset of oxygenic photosynthesis.

MATERIALS AND METHODS

Isolation of Intact PS I Complexes and Preparation of PS I Cores. PS I complexes were isolated from *Synechococcus* sp. PCC 7002 membranes using Triton X-100 and purified by density gradient ultracentrifugation (*7*). The stromal subunits were removed by adding 6.8 M urea to freshly isolated PS I complexes, yielding P_{700}-F_X cores (*5*).

Site-Directed Mutagenesis of the psaC Gene. Site-directed mutants of *psaC* were constructed using a QuikChange site-directed mutagenesis kit (Stratagene, La Jolla, CA). The C-terminal deletion mutant of PsaC was generated by introducing a stop codon (TAA) after the Gly70 codon (GGT). PCR primers were designed on the basis of the sequence of the *psaC* gene from *Synechococcus* sp. PCC 7002. The mutant *psaC* construct was verified by DNA sequencing. The plasmids were subsequently transformed into *Escherichia coli* BL21-DE3 competent cells for protein expression.

Purification and Reconstitution of Recombinant Proteins. Recombinant PsaC (wild-type and variant) and PsaD were expressed in *E. coli* and purified as previously described (*7*). The iron−sulfur clusters were inserted into the PsaC apoprotein by the addition of $FeCl_3$, Na_2S, and 2-mercaptoethanol (*16*). Recombinant flavodoxin from *Synechococcus* sp. PCC 7002 and recombinant cytochrome c_6 from *Synechocystis* sp. PCC 6803 were purified as described previously (*17*, *18*).

Time-Resolved Optical Spectroscopy in the Near-Infrared Region. Optical absorbance changes in the near-infrared region were measured using a laboratory-built spectrophotometer based on a 16-bit A/D converter (National Instruments, Austin, TX) and LabView (*19*). The samples were placed in a quartz cuvette with a path length of 10 mm. The sample contained P_{700}-F_X cores at 50 μg/mL Chl in 50 mM Tris-HCl (pH 8.2), 10 mM sodium ascorbate, 4 μM 2,6-dichlorophenolindophenol (DCPIP), and 0.04% Triton X-100. The samples were prepared in an anaerobic chamber with an atmosphere of 10% hydrogen and 90% nitrogen (Coy Laboratories, Grass Lake, MI). The kinetic traces were analyzed by fitting a multiexponential decay using the Marquardt least-squares algorithm (Igor Pro, Lake Oswego, OR).

Low-Temperature X-Band EPR Spectroscopy. Low-temperature EPR spectroscopy was conducted using a Bruker-ECS 106 X-band spectrometer equipped with an Oxford liquid helium cryostat and temperature controller. The spectrometer conditions were as follows: microwave power, 100 mW; microwave frequency, 9.47 GHz; receiver gain, 20000; modulation amplitude, 20 G at 100 kHz. The signal-to-noise ratio was improved by averaging eight scans. Unbound PsaC samples were exchanged into 100 mM glycine buffer (pH 10.0) and chemically reduced using 10 mM sodium hydrosulfite. All samples that were assayed for light-induced electron transfer contained 10 mM sodium ascorbate and 300 μM DCPIP as the external electron donor and mediator, respectively. Actinic illumination was provided by an argon ion laser, which was operated at 2.0 W in all-lines mode. In all cases, the dark spectrum (sample frozen in darkness) was subtracted from the light-induced spectrum to generate a light-induced difference spectrum of the reduced iron−sulfur clusters.

Steady-State Rates of Flavodoxin Photoreduction. Steady-state rates of light-induced flavodoxin reduction were measured in a 400 μL reaction mixture using cytochrome c_6 as the immediate electron donor to P_{700}. Sodium ascorbate was included as a sacrificial donor. The reaction mixture contained reconstituted PS I complexes at 1.5 μg/mL Chl *a*, 50 mM $MgCl_2$, 5 mM sodium ascorbate, 15 μM cytochrome c_6, and 15 μM flavodoxin. The reduction of flavodoxin was monitored at 467 nm using a Cary 50 Bio UV−visible spectrophotometer with appropriate blocking filters for the actinic and measuring beams. The actinic illumination was provided by high-intensity red light-emitting diodes (Hansatech Instruments).

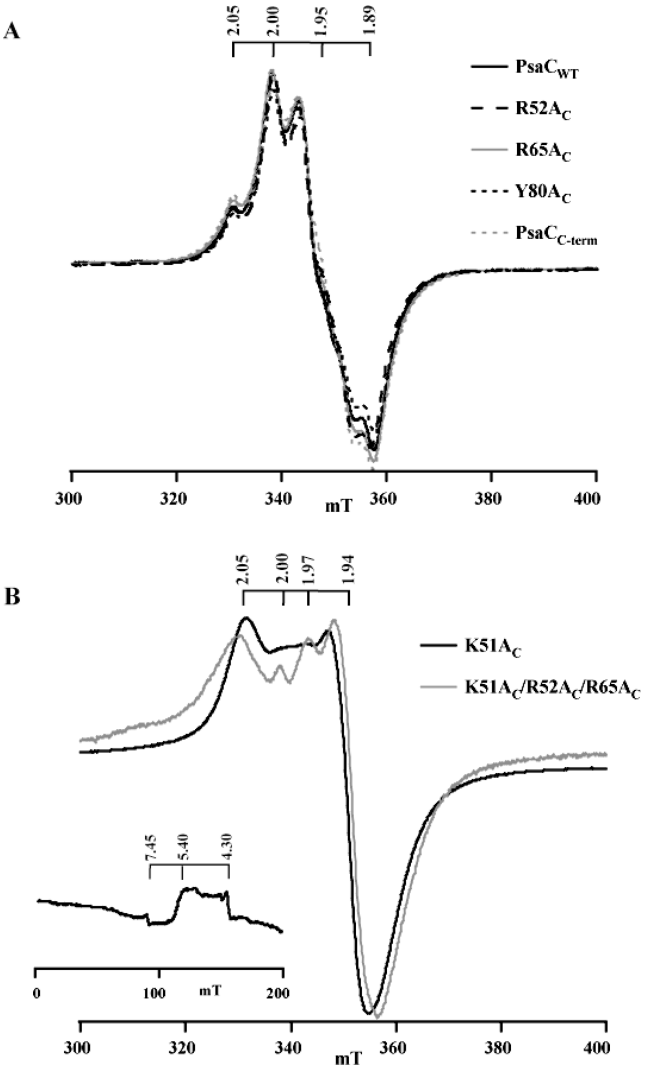

FIGURE 2: EPR spectra of chemically reduced, recombinant PsaC proteins: (A) $PsaC_{WT}$, $R52A_C$, $R65A_C$, $Y80A_C$, and $PsaC_{C\text{-term}}$ and (B) $K51A_C$ and $K51A_C/R52A_C/R65A_C$. The inset of panel B shows low-field resonances characteristic of an $S \geq {}^3/_2$ ground spin state shown in the case of the $K51A_C$ variant. The wild-type and variant PsaC apoproteins were reconstituted with iron−sulfur clusters using the protocol described in Materials and Methods. The sample was reduced with 10 mM sodium hydrosulfite in 100 mM glycine (pH 10.0) buffer. Spectrometer conditions: temperature, 15 K (4.3 K for the inset of panel B); power, 100 mW; microwave frequency, 9.47 GHz; receiver gain, 2000.

RESULTS

Mutagenesis of the psaC Gene. To probe the role of the symmetric ionic contacts between PsaC and the PsaA/PsaB heterodimer, a number of site-directed point mutants of the *psaC* gene were generated. The targeted residues were $R52_C$, which forms all five ionic bonds with $D568_A$ and $D579_A$; $K51_C$, which forms one ionic bond with $D566_B$; and $R65_C$, which forms four of the five ionic bonds with $D555_B$ and $D566_B$ (*14*). In all instances, the basic residue was replaced with an Ala residue ($R52A_C$, $K51A_C$, and $R65A_C$). A $K51A_C/R52A_C/R65A_C$ triple variant was also constructed to eliminate all of the ionic contacts, leaving the nonsymmetric H-bonds intact.

To probe the role of the nonsymmetric H-bonds between PsaC and PsaB, variants were constructed in the C-terminal region of PsaC. $Y80_C$ was previously predicted to play a critical role in the binding process because it forms two of the three H-bonds with PsaB (*20*). A $Y80A_C$ variant was generated to test the prediction that the absence of these H-bonds should prevent PsaC from binding. It has also been proposed that the interaction between a Gly-Leu-Ala-Tyr sequence on the C-terminus of PsaC and a Pro-Val-Ala-Leu hydrophobic pocket on PsaB drives the binding of the two proteins through hydrophobic (i.e., entropic) interactions (*14*, *21*). To test this prediction, the C-terminal deletion variant of PsaC devoid of residues 71−80 and thus lacking all of the symmetry-breaking interactions with PsaB was constructed. This PsaC variant ($PsaC_{C\text{-term}}$) contains only the C_2-symmetric network of ionic contacts.

Low-Temperature EPR Spectroscopy of the Unbound PsaC Variants. Figure 2 shows the EPR spectra of the unbound, chemically reduced wild-type and variant PsaC proteins. The magnetic properties of F_A and F_B depend on the protein environment, with the consequence that an altered EPR spectrum usually reflects a change in structure. The $R52A_C$, $R65A_C$, $Y80A_C$, and $PsaC_{C\text{-term}}$ variants exhibit a typical F_A^-/F_B^- magnetic

interaction spectrum with resonances at apparent g values of 2.05, 2.00, 1.95, and 1.89 (Figure 2A). The resonances are nearly identical to those in wild-type PsaC ($PsaC_{WT}$). Given the high degree of similarity of the EPR spectra, we can conclude that the amino acid changes do not significantly affect the magnetic properties of the F_A and F_B iron−sulfur clusters. Hence, the structural integrity of the variant proteins appears to be well-maintained in spite of the altered residues.

In contrast, the $K51A_C$ variant and the $K51A_C/R52A_C/R65A_C$ triple variant show a simple, axial-like spectrum (Figure 2B) that is usually found in proteins that contain a single $S = {}^1/_2$ [4Fe-4S] cluster or in dicluster ferredoxins that contain an $S = {}^1/_2$ [4Fe-4S] cluster in one site and an $S \geq {}^3/_2$ [4Fe-4S] cluster in the other site (*22*). A search at very low temperatures and high microwave powers for the presence of an $S \geq {}^3/_2$ [4Fe-4S] cluster yielded resonances between $g = 5$ and 8 characteristic of a high-spin ground state (in the inset of Figure 2B, note that the amplitudes of the resonances are one-tenth that of the $g \sim 2$ resonances). Thus, it appears that the magnetic properties of the iron−sulfur clusters are altered such that one remains in the $S = {}^1/_2$ ground spin state and the other assumes an $S \geq {}^3/_2$ ground spin state.

Charge Recombination Kinetics of Reconstituted P_{700}-F_X/Variant PsaC Complexes. In native PS I complexes, charge recombination between P_{700}^+ and $[F_A/F_B]^-$ occurs with a lifetime of 60−80 ms. Upon the removal of PsaC (and hence F_A and F_B), charge recombination occurs between P_{700}^+ and F_X^- with a lifetime of 1−2 ms. During the preparation of P_{700}-F_X cores, a small population of P_{700}-A_1 cores is formed due to the inadvertent degradation of the F_X cluster. Because PsaC cannot bind in the absence of the F_X cluster (*23*), the small fraction of P_{700}-A_1 complexes continues to undergo charge recombination between P_{700}^+ and A_1^- with a lifetime of 10 μs, which accounts for ~10% of the absorbance decay after the flash-induced formation of P_{700}^+. For the sake of clarity, this fast recombination between P_{700}^+ and A_1^- is not shown in the decay kinetics of the P_{700}-F_X/variant PsaC complexes.

As shown in Figure 3A, ~75% of the charge recombination between P_{700}^+ and $[F_A/F_B]^-$ is restored upon the addition of a 1.5-fold molar excess of recombinant $PsaC_{WT}$ to P_{700}-F_X cores. The further addition of PsaD does not influence the charge recombination kinetics (data not shown). There is a small contribution to the decay (lifetime, 1500 ms; amplitude, 15%) due to forward donation of electrons from DCPIP to P_{700}^+ in PS I complexes that have lost an electron from $[F_A/F_B]^-$. Although all samples were prepared under anaerobic conditions, trace amounts of oxygen may be sufficient to accept electrons from $[F_A/F_B]^-$. In these samples, the primary donor, P_{700}^+, is slowly reduced by the exogenous electron donor, DCPIP, in a time range of seconds.

$R52_C$ forms three ionic bonds with $D579_A$ and two ionic bonds with $D568_A$ for a total of five ionic bonds with the PsaA protein. Figure 3B shows the charge recombination kinetics after the addition of a 10-fold excess of $R52A_C$ to P_{700}-F_X cores. The dominant kinetic phase (lifetime of ~2 ms, amplitude of 65%) represents charge recombination between P_{700}^+ and F_X^- and therefore corresponds to a fraction of P_{700}-F_X cores that do not bind $R52A_C$. An additional kinetic phase (lifetime of ~500 ms, amplitude of 25%) may be due to charge recombination between P_{700}^+ and $[F_A/F_B]^-$. (These kinetics may represent an admixture with that of donation of DCPIP to P_{700}^+ in PS I complexes that have lost an electron from $[F_A/F_B]^-$.) The addition of PsaD (Figure 3C) results in the appearance of an ~50 ms kinetic phase (amplitude of 40%), which can be attributed to the charge recombinant kinetics between P_{700}^+ and $[F_A/F_B]^-$. Thus, PsaD imparts native PS I-like kinetics to a significant fraction of the P_{700}-$F_X/R52A_C$ complexes. To the best of our knowledge, this represents the first instance in which the presence of PsaD has been found to influence the lifetime of the charge-separated state in PS I.

$R65_C$ forms two ionic bonds with $D555_B$ and two ionic bonds with $D566_B$ for a total of four ionic bonds with the PsaB protein. Figure 3D shows the charge recombination kinetics after the addition of a 10-fold excess of $R65A_C$ to P_{700}-F_X cores. The kinetics are similar to those found in P_{700}-$F_X/R52A_C$ complexes, showing lifetimes of ~2 ms (70%) and ~500 ms (20%). However, unlike the case for the P_{700}-$F_X/R52A_C$ complexes, the addition of PsaD results in no additional changes (data not shown).

The addition of the $K51A_C$ or $K51A_C/R52A_C/R65A_C$ variant to P_{700}-F_X cores resulted in no alteration of the ~2 ms kinetic phase attributed to charge recombination between P_{700}^+ and F_X^- (data not shown). The addition of PsaD resulted in no further changes. It is noteworthy that these variant PsaC proteins exhibit non-native EPR spectra in the unbound state, reflecting most likely a significant change in their three-dimensional structures.

Figure 3E shows the charge recombination kinetics after the addition of $Y80A_C$ to P_{700}-F_X cores. Surprisingly, the kinetics are similar to those of the reconstituted P_{700}-$F_X/PsaC_{WT}$ complexes, which suggests that the absence of the two H-bonds to PsaB does not significantly affect the binding of $Y80A_C$. However, addition of a 3-fold molar excess of $Y80A_C$ to P_{700}-F_X cores was required to achieve the maximum effect, as compared to a 1.5-fold molar excess of $PsaC_{WT}$. The addition of PsaD resulted in no additional changes (data not shown).

Figure 3F shows the charge recombination kinetics after the addition of the $PsaC_{C\text{-}term}$ variant to P_{700}-F_X cores. Despite the addition of a 10-fold excess, a significant fraction of P_{700}-F_X complexes retain the ~2 ms kinetic phase (amplitude of 40%), which indicates that they do not rebind $PsaC_{C\text{-}term}$. A nearly equivalent fraction (amplitude of 50%) showed charge recombination kinetics greater than 800 ms, which might originate from bound $PsaC_{C\text{-}term}$. The addition of PsaD resulted in no additional changes (data not shown).

It should be noted that the amplitude of the flash-induced absorption change at 820 nm is the same in all P_{700}-F_X/variant PsaC complexes, indicating that the relative amount of long-lived (i.e., > 1 ms) P_{700}^+ formed is nearly identical in all the samples.

Low-Temperature EPR Spectroscopy of Illuminated P_{700}-F_X/Variant PsaC Complexes. The slower kinetic phases (those with lifetimes greater than 500 ms) could arise either from donation of DCPIP to P_{700}^+ in PS I complexes that have lost an electron from $[F_A/F_B]^-$ or from charge recombination between $[F_A/F_B]^-$ and P_{700}^+. We conducted low-temperature EPR spectroscopy to verify electron transfer to F_A and F_B and thus to clarify the origin of the slower kinetic phases. Additionally, EPR spectroscopy provides information about the magnetic environment of F_A and F_B during the different stages of PS I assembly. In native PS I, freezing a sample in the dark with subsequent illumination at 15 K allows promotion of one electron from P_{700} to either F_A or F_B, but not both, in a given PS I complex (*24*). Under these conditions, the resulting EPR spectrum is a superimposition of the resonances from F_A^- (g values of 2.05, 1.95, and 1.85) and F_B^- (g values of 2.09, 1.93, and 1.88). P_{700}-F_X cores

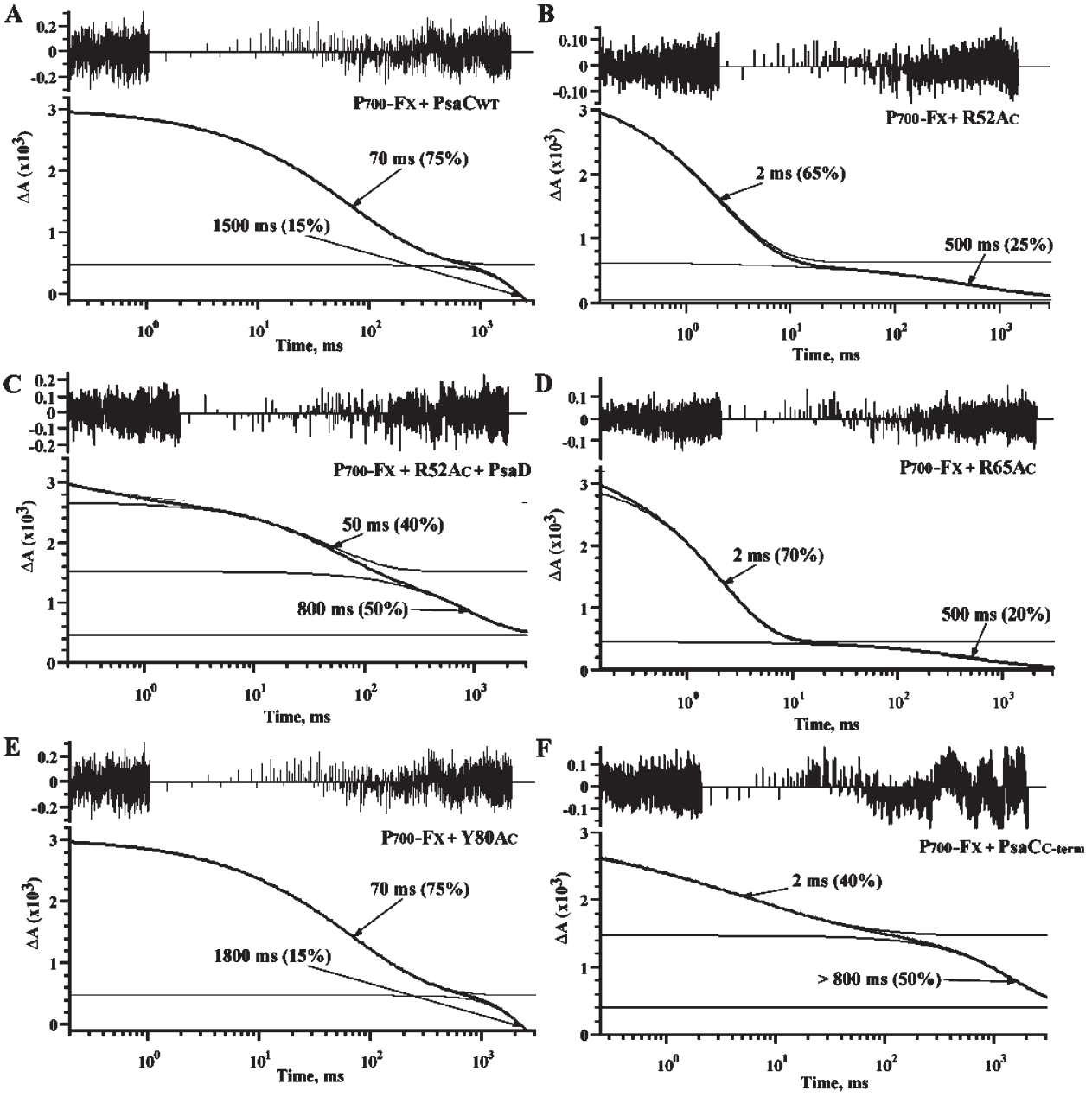

FIGURE 3: Flash-induced absorption changes of P_{700}^+ reduction monitored at 820 nm in (A) P_{700}-F_X/$PsaC_{WT}$, (B) P_{700}-F_X/$R52A_C$, (C) P_{700}-F_X/$R52A_C$/PsaD, (D) P_{700}-F_X/$R65A_C$, (E) P_{700}-F_X/$Y80A_C$, and (F) P_{700}-F_X/$PsaC_{C\text{-term}}$ complexes. The PS I core concentration was 50 μg/mL Chl *a*. All samples contained 10 mM sodium ascorbate and 4 μM DCPIP as the electron donor and mediator, respectively.

do not exhibit strong EPR resonances from F_X^- at the temperatures employed for this measurement, but they retain the $g = 2.00$ feature from the oxidized primary donor, P_{700}^+.

The EPR spectrum of reconstituted P_{700}-F_X/$PsaC_{WT}$ complexes that were frozen in the dark with subsequent illumination at 15 K shows resonances at *g* values of 2.07, 2.03, 1.97, 1.94, and 1.87 (Figure 4A). The individual resonances are considerably broader than those in native PS I complexes. The addition of PsaD causes the resonances to sharpen, assuming line widths approaching that of F_A^- and F_B^- in native PS I complexes (data not shown) (*7*).

Figure 4B shows the EPR spectrum of P_{700}-F_X/$R52A_C$ complexes after illumination at 15 K. The *g* values of the resonances are similar to those of the P_{700}-F_X/$PsaC_{WT}$ complexes. The detection of light-induced EPR resonances indicates that electron transfer to F_A/F_B occurs even at low temperatures. Thus, the ~500 ms kinetic phase observed at room temperature can likely be attributed to the charge recombination between P_{700}^+ and $[F_A/F_B]^-$. The alteration in the EPR spectrum of the P_{700}-F_X/$R52A_C$ complexes compared to that of the P_{700}-F_X/$PsaC_{WT}$ complexes signifies a change in the environment of the F_A and F_B clusters. The addition of PsaD sharpens the EPR resonances in the reconstituted P_{700}-F_X/$R52A_C$ complexes, resulting in line widths similar to that of native PS I (Figure 4C). The alteration of the EPR spectrum in the presence of PsaD correlates with a change in the room-temperature charge recombination kinetics described earlier.

The P_{700}-F_X/$R65A_C$ complexes fail to exhibit light-induced resonances of F_A and F_B, in spite of the fact that one PsaC−PsaB ionic bond remains intact between $K51_C$ and $D566_B$. The addition of PsaD results in no additional changes. However, when the P_{700}-F_X/$R65A_C$/PsaD complexes were illuminated during freezing, low-amplitude resonances were observed at *g* values of 2.05, 2.02, 1.97, 1.94, and 1.88 (Figure 4D).

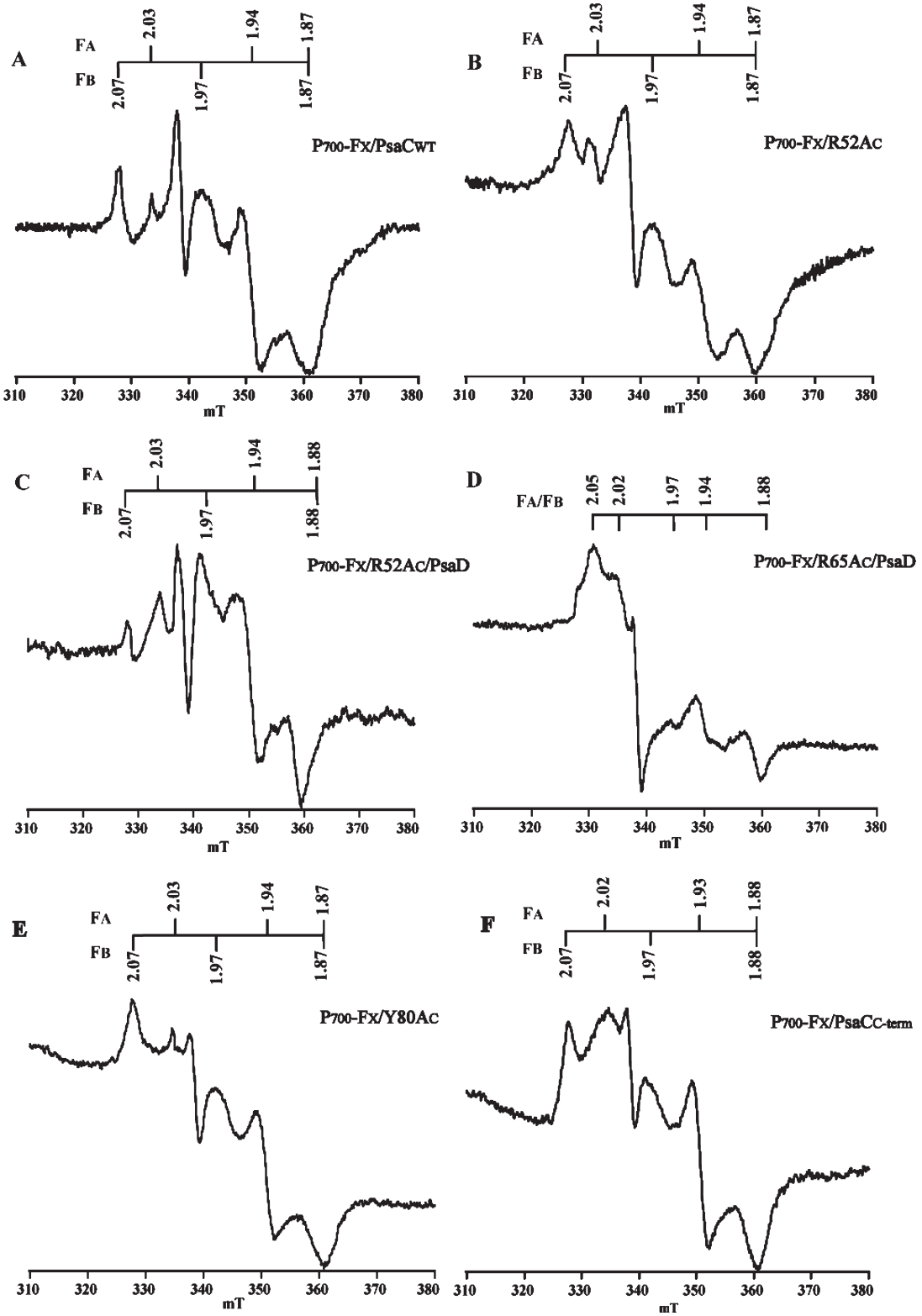

FIGURE 4: Light-induced EPR spectra of (A) P_{700}-F_X/PsaC$_{WT}$, (B) P_{700}-F_X/R52A$_C$, (C) P_{700}-F_X/R52A$_C$/PsaD, (D) P_{700}-F_X/R65A$_C$/PsaD, (E) P_{700}-F_X/Y80A$_C$, and (F) P_{700}-F_X/PsaC$_{C\text{-term}}$ complexes. The samples contained 10 mM sodium ascorbate and 300 μM DCPIP as the electron donor and mediator, respectively. Samples A−C, E, and F were frozen in the dark and illuminated in-cavity at 15 K using an argon ion laser. Sample D was illuminated during freezing to 77 K in a glass dewar. The spectra depicted are the differences between the illuminated and dark-adapted samples. Spectrometer conditions: temperature, 15 K; power, 100 mW; microwave frequency, 9.47 GHz; receiver gain, 20000. The isotropic g = 2.00 signal due to P_{700}^+ is distorted due to the low temperature and high modulation amplitude required to detect the iron−sulfur clusters.

Freezing intact PS I complexes during illumination promotes multiple electron transfers, leading to the reduction of both F_A and F_B. The magnetic coupling between the reduced F_A and F_B clusters results in an interaction spectrum with g values that differ from the simple sum of the individual spectra of F_A^- and F_B^- (*24*). However, the resulting weak EPR spectrum of P_{700}-F_X/R65A$_C$/PsaD complexes is slightly different from that of native PS I and is consistent with a low quantum yield of reduction of the F_A and F_B clusters.

Table 1: Steady-State Rates of Flavodoxin Photoreduction Measured for P_{700}-F_X/Variant PsaC/PsaD Complexes Using Ascorbate/Cytochrome c_6 as the Electron Donor[a]

	rate of flavodoxin photoreduction [μmol (mg of Chl)$^{-1}$ h^{-1}]			
complex	0 h	16 h	32 h	48 h
native PS I	450	440	455	435
P_{700}-F_X core	0	0	0	0
P_{700}-F_X/$PsaC_{WT}$/PsaD	360	350	345	350
P_{700}-F_X/$R52A_C$/PsaD	270	270	260	255
P_{700}-F_X/$R65A_C$/PsaD	125	115	115	120
P_{700}-F_X/$Y80A_C$/PsaD	300	290	295	305
P_{700}-F_X/$PsaC_{C\text{-}term}$/PsaD	195	180	185	180

[a] The rates were obtained using an aliquot of the rebuilt complexes that were initially assayed for light-induced EPR activity and kept under strictly anaerobic conditions. The samples were rapidly transferred from the EPR tube into a cuvette with a path length of 10 mm, thus ensuring minimum exposure to oxygen (0 h). The rates of flavodoxin photoreduction were measured at several time points over 48 h, during which the samples were maintained under strictly anaerobic conditions.

As expected, the addition of $K51A_C$ or $K51A_C$/$R52A_C$/$R65A_C$ to P_{700}-F_X cores did not result in the appearance of resonances from F_A or F_B when the sample was illuminated at 15 K or frozen under illumination (data not shown). The addition of PsaD led to no additional changes. These findings agree with the room-temperature charge recombination data, wherein no charge recombination is observed between P_{700}^+ and $[F_A/F_B]^-$.

The EPR spectrum of P_{700}-F_X/$Y80A_C$ complexes is almost identical to that of P_{700}-F_X/$PsaC_{WT}$ complexes (Figure 4E), a finding consistent with the room-temperature charge recombination data. Not surprisingly, the EPR spectrum of the P_{700}-F_X/$Y80A_C$/PsaD complex is identical to that of the P_{700}-F_X/$PsaC_{WT}$/PsaD complex (data not shown), further indicating that the absence of the two H-bonds between PsaC and PsaB does not significantly influence the assembly of PsaC onto P_{700}-F_X cores.

Figure 4F shows the EPR spectrum of P_{700}-F_X/$PsaC_{C\text{-}term}$ complexes after illumination at 15 K. The resonances detected at g values of 2.07, 2.02, 1.97, 1.93, and 1.88 are slightly different from the resonances observed in P_{700}-F_X/$PsaC_{WT}$ complexes. Thus, the absence of the C-terminus does not preclude the binding of variant PsaC to P_{700}-F_X cores or electron transfer to F_A and F_B. The addition of PsaD resulted in no additional changes (data not shown), a finding consistent with the charge recombination kinetic data.

It is difficult to accurately quantitate the EPR signals of F_A^- and F_B^-, given the signal-to-noise ratio, the complexity of the spectral features, and the broad line widths of the resonances. However, an attempt was made to compare the relative intensities of the midfield resonances to estimate the efficiency of light-induced charge separation to F_A^-/F_B^- at low temperatures. On the basis of the qualitative comparison, we arranged the PsaC variants according to the degree of reduction of F_A/F_B in the following order: $PsaC_{WT} \gg Y80A_C \gg R52A_C$/PsaD $\gg PsaC_{C\text{-}term} \gg R52A_C \gg R65A_C$/PsaD. This trend is in good agreement with the relative amplitudes of the charge recombination phase between P_{700}^+ and $[F_A/F_B]^-$ in the P_{700}-F_X/variant PsaC complexes.

Steady-State Rates of Light-Induced Flavodoxin Reduction. The throughput of electron transfer was studied at room temperature in the reconstituted PS I complexes by measuring the steady-state rates of flavodoxin reduction using ascorbate/cytochrome c_6 as the electron donor (Table 1). At the actinic light intensity employed in this experiment, native PS I complexes support a light-induced rate of flavodoxin reduction of 450 μmol (mg of Chl)$^{-1}$ h^{-1}, whereas P_{700}-F_X cores fail to show any measurable activity. Reconstituted P_{700}-F_X/$PsaC_{WT}$/PsaD complexes support a rate of 360 μmol (mg of Chl)$^{-1}$ h^{-1}. The slightly lower rate relative to that of the wild type is partly due to the inability of PsaC to bind to P_{700}-A_1 cores that are devoid of the F_X cluster. P_{700}-F_X/$R52A_C$/PsaD complexes and P_{700}-F_X/$R65A_C$/PsaD complexes support rates of 270 and 125 μmol (mg of Chl)$^{-1}$ h^{-1} respectively. The relatively low rate of light-induced flavodoxin reduction observed with $R65A_C$ is consistent with both the kinetic and EPR data. The P_{700}-F_X complexes that were reconstituted with $Y80A_C$ and $PsaC_{C\text{-}term}$ support rates of 300 and 195 μmol (mg of Chl)$^{-1}$ h^{-1}, respectively. It is clear that the absence of $Y80_C$ does not significantly affect the rate of light-induced flavodoxin reduction, but the removal of the entire C-terminus results in a significant loss of activity. In all cases, the native PS I and reconstituted P_{700}-F_X/variant PsaC/PsaD complexes retain between 90 and 95% of their original steady-state rates of flavodoxin photoreduction for at least 48 h when kept under strictly anaerobic conditions (Table 1).

The [4Fe-4S] clusters in unbound PsaC are sensitive to degradation by dioxygen as a result of insufficient shielding by protein (*14*). When docked onto PS I cores in the presence of PsaD, the [4Fe-4S] clusters of PsaC are stable in the presence of dioxygen. However, the PsaC variant proteins may not bind in a native configuration to P_{700}-F_X cores, and the F_A and F_B clusters in P_{700}-F_X/variant PsaC complexes may therefore retain some sensitivity to oxidative denaturation. To test this idea, steady-state rates of light-induced flavodoxin reduction were measured at several time points during a 48 h dark exposure of the original samples to atmospheric dioxygen (Table 2). Over the course of a 48 h exposure, 95 and 90% of the original rate of flavodoxin reduction are retained in native PS I complexes and reconstituted P_{700}-F_X/$PsaC_{WT}$/PsaD complexes, respectively. In contrast, only 20% of the original rate of flavodoxin reduction is retained in reconstituted P_{700}-F_X/$R52A_C$/PsaD complexes over the same time period. The decline is even more pronounced in P_{700}-F_X/$R65A_C$/PsaD complexes, which retain only 10% of the original rate of flavodoxin reduction after 32 h. The greater sensitivity of the $R65A_C$ variant compared to the $R52A_C$ variant correlates with the spectroscopic data described earlier.

Over the course of a 48 h exposure, 70 and 50% of the rate of flavodoxin reduction are retained in P_{700}-F_X/$Y80A_C$/PsaD and P_{700}-F_X/$PsaC_{C\text{-}term}$/PsaD complexes, respectively. Thus, the absence of the C-terminal contacts of PS I-bound PsaC renders the F_A/F_B clusters sensitive to oxidative denaturation, although the effect is less pronounced than when one of the symmetric ionic

Table 2: Steady-State Rates of Flavodoxin Photoreduction Measured for P_{700}-F_X/Variant PsaC/PsaD Complexes Described in Table 1 after Exposure to Atmospheric Oxygen at 4 °C in the Dark[a]

	rate of flavodoxin photoreduction [μmol (mg of Chl)$^{-1}$ h^{-1}]			
complex	0 h	16 h	32 h	48 h
native PS I	435	450	445	440
P_{700}-F_X core	0	0	0	0
P_{700}-F_X/$PsaC_{WT}$/PsaD	350	350	335	325
P_{700}-F_X/$R52A_C$/PsaD	255	170	100	55
P_{700}-F_X/$R65A_C$/PsaD	120	55	15	0
P_{700}-F_X/$Y80A_C$/PsaD	305	250	225	210
P_{700}-F_X/$PsaC_{C\text{-}term}$/PsaD	180	160	135	95

[a] The original samples were exposed to dioxygen for 48 h after being kept under strictly anaerobic conditions. The 0 h time point corresponds to the 48 h time point of Table 1.

contacts is missing. Hence, although the H-bonds from $Y80_C$ do not affect the binding of PsaC, they play a role in stabilizing PsaC by protecting the [4Fe-4S] clusters against denaturation by dioxygen.

DISCUSSION

Altered Charge Recombination Kinetics. With one exception, the reconstituted PS I complexes with variant PsaC proteins exhibit slower charge recombination kinetics between P_{700}^+ and $[F_A/F_B]^-$ than the wild type. Before we discuss the details of recombination kinetics, we briefly review the parameters that govern the rate of electron transfer in proteins. According to Marcus theory, the rate of electron transfer between a donor and acceptor pair is a function of two independent parameters (*25*).

One parameter is the Franck−Condon factor, which relates the change in Gibbs free energy between the donor−acceptor pair, the reorganization energy, and the temperature to the rate of electron transfer. The time-resolved optical experiments reported here were conducted at a constant temperature. The reorganization energy is assumed to be a relatively constant 0.7 eV in proteins, although a value of 1.0 has been estimated for the kinetics of electron transfer from A_1 to F_X (*26*). The change in Gibbs free energy depends on the midpoint potentials of F_X and F_A/F_B, which in turn depend on the protein environment. Although the function of the protein environment in modulating the midpoint potentials of iron−sulfur clusters is incompletely understood, solvent accessibility and the orientation of charged amino acids around the cluster are thought to play a major role (*27*). It should be noted, however, that the charge recombination kinetics between P_{700}^+ and $[F_A/F_B]^-$ represents a more complicated situation than simple electron transfer between a donor−acceptor pair. The process most likely involves quasi-equilibrium between the electron acceptors and in the wild type proceeds by thermal repopulation of F_X^- and most probably A_{1A}^-/A_{1B}^- (*28*, *29*). The rate of recombination is driven by the ΔG between F_X^- and $[F_A/F_B]^-$, by the ΔG between A_{1A}^-/A_{1B}^- and F_X^-, and by direct electron transfer from A_{1A}^-/A_{1B}^- to P_{700}^+, with the necessary precondition of quasi-equilibrium between the redox pairs. A change in rate in a P_{700}-F_X/variant PsaC complex may thus reflect a change in ΔG, which is just another way of stating an equilibrium constant with its attendant forward and backward rate constants. Thus, an altered reduction potential of the iron−sulfur clusters would result in a different rate of thermalization of the electron acceptor chain, manifest in this study as a slower rate of charge recombination of $[F_A/F_B]^-$ with P_{700}^+.

The other parameter is the matrix coupling element, which relates the distance between the donor−acceptor pair to the rate of electron transfer. The edge-to-edge distance between the donor−acceptor pairs has a profound influence on the rate of electron transfer; in proteins, there is a predicted 10-fold change in the rate for every 1.7 Å change in distance (*30*). The PS I crystal structure (Protein Data Bank entry 1JB0) shows that F_X and F_A are located ~15 Å (center to center) from each other, a distance that ensures a fast rate of forward electron transfer relative to the rate of charge recombination between P_{700}^+ and F_X^-. A longer distance would result in a slower rate of electron transfer between $[F_A/F_B]^-$ and F_X, which would result in a slower rate of thermalization of the electron acceptor chain. This would also manifest itself as slower rate of charge recombination of $[F_A/F_B]^-$ with P_{700}^+.

In the absence of structural information for the P_{700}-F_X/variant PsaC complexes, it is difficult to attribute the altered charge recombination rates to a change in ΔG or a change in distance. Given that the mutations introduced into PsaC affect its binding to the PsaA/PsaB heterodimer as shown by low-temperature EPR spectroscopy, and given the exceedingly high sensitivity of electron transfer rate to distance, the alteration in the charge recombination kinetics of reconstituted PS I complexes may result from a subtle change in the distance between F_X and F_A/F_B as well as from a change in the redox potential(s) of the iron−sulfur clusters.

Analysis of Contacts between PsaC and the PsaA/PsaB Heterodimer. One unexpected finding was that the replacement of a positively charged Lys residue with a neutral Ala residue influences the magnetic coupling of the iron atoms within the affected [4Fe-4S] cluster of the $K51A_C$ variant, leading to the appearance of an $S \geq {}^3/_2$ ground spin state. Although the factors that govern the coupling of the ferrous and ferric atoms in [4Fe-4S] clusters are incompletely understood (see refs (*31*) and (*32*) for reviews), the protein environment plays a crucial role in determining the most energetically favorable ground spin state. It has long been known that when the second cysteine residue in the CxxCxxCxxxCP motif that ligates the [4Fe-4S] clusters in PsaC is missing, an $S > {}^1/_2$ ground spin state occurs (*33*). One way to accomplish this is to substitute a Ser or an Asp residue for the Cys residue (*34*, *35*); another is to substitute a Gly residue, with the result that 2-mercaptoethanol is retained when a synthetic [4Fe-4S] cluster is inserted into the *E. coli*-expressed PsaC apoprotein (*22*, *36*). Because there are no nearby Ser or Asp residues available to serve as a substitute ligand, we suggest that the substitution of Lys for Ala in position 51 has altered the

protein folding such that a 2-mercaptoethanol is retained during the ligand exchange process. The implication is that one of the protein-bound Cys residues, which would normally displace the 2-mercaptoethanol, is unable to do so for steric reasons. The altered ground spin state could therefore reflect an altered three-dimensional structure, which in the case of $K51A_C$ would be sufficiently different from native PsaC to preclude binding to the PsaA/PsaB heterodimer. Additionally, if the 2-mercaptoethanol were to provide the ligand to one of the iron atoms, its presence may sterically hinder the binding of the variant to the PsaA/PsaB heterodimer.

$R65_C$ is involved in the remaining four of the five symmetry-related ionic contacts with PsaB (*14*). The absence of electron transfer between F_X and F_A when $R65A_C$ is added to P_{700}-F_X cores demonstrates the importance of these crucial binding contacts. The loss of electron transfer can be attributed to altered binding or, alternatively, to a complete inability of $R65A_C$ to bind to P_{700}-F_X cores. The former would involve either increasing the distance between F_X and F_A or altering their redox potentials such that charge recombination between P_{700}^+ and F_X^- would outcompete forward electron transfer from F_X^- to F_A/F_B. The addition of PsaD to P_{700}-F_X/$R65A_C$ complexes results in a weak set of EPR resonances from F_A^-/F_B^-, but they are only visible after a multiple-turnover photoaccumulation protocol. It is possible that in a small fraction of the reconstituted PS I complexes, PsaD clamps $R65A_C$ tightly onto the P_{700}-F_X core, thereby decreasing the distance between F_X and F_A or altering their redox potentials, thereby allowing forward electron transfer to outcompete charge recombination.

$R52_C$ participates in five ionic bonds with PsaA and is responsible for one-half of the symmetry-related contacts between PsaC and the PsaA/PsaB heterodimer (*14*). Unlike the complex with $R65_C$, the P_{700}-F_X/$R52A_C$ complex is able to support electron transport to F_A and F_B, albeit with a charge recombination rate slower that that of native PS I complexes. Interestingly, the addition of PsaD imparted native PS I-like properties to a significant fraction of the P_{700}-F_X/$R52A_C$ complexes. In the 2.5 Å X-ray crystal structure of PS I (Protein Data Bank entry 1JB0), the C-terminus of PsaD has extensive interactions with the N-terminus of PsaC, which is positioned very close to the F_A cluster (*11*, *14*). Because $R52_C$ is part of the F_A-coordinating CxxCxxCxxxCP motif, it seems possible that the absence of the PsaC−PsaA contacts is compensated to some degree by the extensive PsaC−PsaD contacts.

Computational studies involving a geometric simulation algorithm have predicted that the C-terminus of PsaC binds first to the specific binding pocket on PsaB (*20*). The algorithm simulates large-scale motions in proteins and was used to provide a snapshot of possible intermediates in the binding of PsaC. It was proposed that $Y80_C$ is critical to the binding process, given that it forms two of the three symmetry-breaking hydrogen bonds with PsaB (*20*). However, on the basis of our studies, it appears that $Y80_C$ is not essential for PsaC binding, although it may add to the strength of the interactions between the C-terminus of PsaC and PsaB.

It has also been proposed that hydrophobic interactions between a Gly-Leu-Ala-Tyr sequence on the C-terminus of PsaC and a Pro-Val-Ala-Leu sequence on PsaB drive the binding of the two subunits (*14*, *21*). A PsaC variant that lacks the C-terminus (residues 71−80) still binds to P_{700}-F_X cores, although the reconstituted P_{700}-F_X/$PsaC_{C\text{-}term}$ complexes exhibit markedly slower charge recombination kinetics than native PS I complexes. The C-terminus of PsaC is longer than in typical bacterial dicluster ferredoxins and is proposed to be involved in the initial stages of PsaC assembly, wherein it locates the hydrophobic binding pocket on PsaB (*14*, *21*). It appears from our studies that the interactions between PsaB and the C-terminus of PsaC are necessary to attain a native conformation. We therefore conclude that the symmetric ionic bonds in the vicinity of the F_X cluster are by themselves not sufficient for PsaC to bind in a native configuration on the P_{700}-F_X core.

Factors Contributing to the Oxygen Stability of PS I-Bound PsaC. (i) Structural Features. It has been proposed that the sensitivity to dioxygen of the [4Fe-4S] clusters in unbound PsaC is a result of inadequate shielding at its N-terminus, which is positioned perpendicular to the pre-C-terminus (residues 62−68) and away from the F_A cluster (*14*, *16*). In PS I-bound PsaC, the N-terminus is parallel to the C-terminus and positioned closer to the F_A cluster. It forms an antiparallel β-sheet with the pre-C-terminus, a motif typical of most bacterial dicluster ferredoxins (*37*). Because of the long C-terminal extension, the pre-C-terminus of PsaC is the only region that corresponds to the C-terminus of typical bacterial ferredoxins. It should be noted that the N-terminus of PsaC contains a minor extension of two amino acids when compared to typical dicluster ferredoxins. The rearrangement of the N-terminus has been predicted to provide better shielding to the F_A cluster and prevent oxidative degradation of the [4Fe-4S] clusters in PS I-bound PsaC (*14*). To the best of our knowledge, the [4Fe-4S] clusters in all known dicluster bacterial ferredoxins are oxygen-sensitive. The antiparallel β-sheet between the N- and C-termini is present in the dicluster ferredoxins from *Clostridium pasteurianum* and *Peptococcus aerogenes* (*38*, *39*), yet their [4Fe-4S] clusters degrade rapidly under aerobic conditions (*40*, *41*). Their structures (Protein Data Bank entries 1CLF and 1DUR) (Figure 5A,B) show that a bridging μ-sulfido atom of the F_A-like cluster is solvent-exposed despite the proximity of the N-terminus and thus may be susceptible to oxidation by dioxygen (*42*). The F_A cluster in unbound PsaC (Protein Data Bank entry 1K0T) also contains a bridging sulfide atom that seems to be relatively poorly shielded by the protein (Figure 5C). It appears from the X-ray crystal structure of PS I-bound PsaC (Protein Data Bank entry 1JB0) that the minor extension of the N-terminus and the extended C-terminus act as a steric barrier that prevents access and thus stabilizes the [4Fe-4S] cluster under aerobic conditions (Figure 5D). The 50% decrease in the light-induced rates of flavodoxin reduction observed after the P_{700}-F_X/$PsaC_{C\text{-}term}$/PsaD complexes have been exposed to oxygen is consistent with the proposal that the C-terminus plays a role equally as important as that of the N-terminus in the oxygen stability of the [4Fe-4S] clusters. In the absence of the extended C-terminus, the structure of PsaC in the vicinity of the F_A cluster is likely very similar to typical dicluster ferredoxins, with the bridging sulfide atom relatively more solvent exposed.

(ii) Binding Interface. This study shows that the extensive network of symmetric ionic contacts and asymmetric hydrogen bonds is necessary for positioning PsaC on the PsaA/PsaB heterodimer so as to support high rates of electron transfer from P_{700} to the F_A/F_B clusters. These contacts also ensure that the association between the protein subunits is extremely tight, thereby rendering the binding interface inaccessible to solvent and/or dioxygen. The latter would serve as an electron acceptor, and its ability to oxidize the bridging μ-sulfido atoms would initiate the degradation of the [4Fe-4S] clusters in PsaC (*42*).

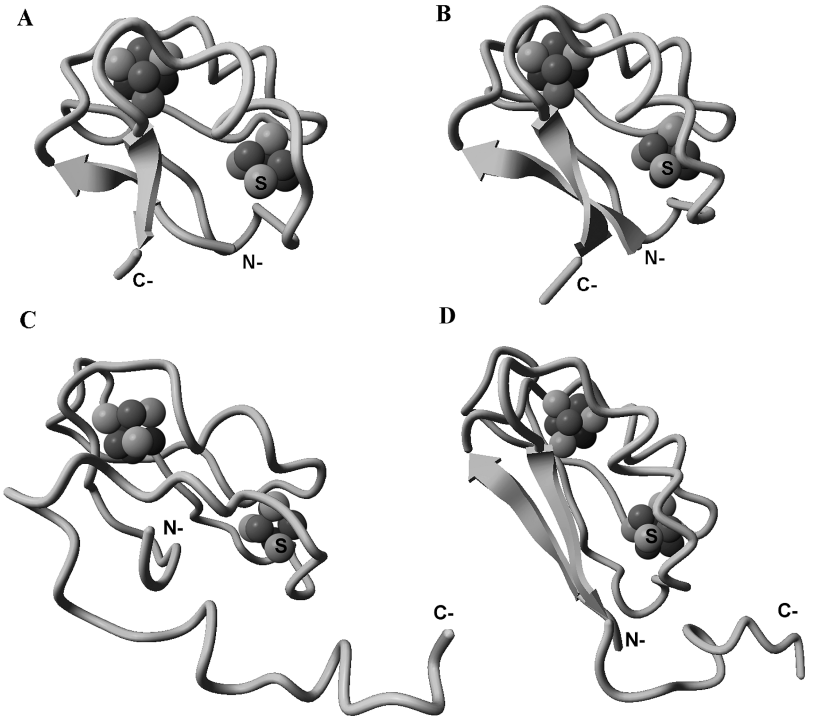

FIGURE 5: Structures of (A) *C. pasteurianum* ferredoxin (Protein Data Bank entry 1CLF), (B) *P. aerogenes* ferredoxin (Protein Data Bank entry 1DUR), (C) unbound PsaC (Protein Data Bank entry 1K0T), and (D) PS I-bound PsaC (Protein Data Bank entry 1JB0). The termini (N- and C-) and the solvent-exposed bridging μ-sulfido atoms (S) are indicated. The view for PS I-bound PsaC is shown from the perspective of the F_X cluster. The F_A cluster in PS I-bound PsaC is likely protected against oxidative degradation by three features: a minor N-terminal extension of two amino acids, the extended C-terminus, and the tight binding of the protein with the PsaA/PsaB heterodimer.

In support of this idea, the P_{700}-F_X/variant PsaC/PsaD complexes supported lower rates of flavodoxin photoreduction after exposure to dioxygen, most likely due to the degradation of the F_A and F_B clusters. The altered binding of the variant PsaC proteins may not provide the level of shielding at the PsaC−PsaA/PsaB interface that is required to protect the [4Fe-4S] clusters from dioxygen.

The F_A cluster may be more sensitive to oxidative denaturation than the F_B cluster, if only because the latter appears to be better shielded by protein (*16*). Because all of the symmetric ionic contacts between PsaC and the PS I core are formed in the vicinity of the F_A cluster, the removal of these contacts may render this [4Fe-4S] cluster particularly susceptible to oxidative denaturation. The absence of $R65_C$ shows the strongest effect; the reconstituted P_{700}-F_X/$R65A_C$/PsaD complexes lose their ability to reduce flavodoxin at a faster rate than the other PsaC variants. The degradation of the F_A/F_B clusters should proceed even faster in a living cell that is actively engaged in photosynthesis and is thus supersaturated with dioxygen.

In work that was conducted prior to the elucidation of the 2.5 Å X-ray crystal structure of PS I, Fischer and colleagues (*43*) addressed the role of $K52_C$ and $R53_C$ in a series of PsaC variants generated in vivo in *Chlamydomonas reinhardtii*. They found that the $K52S_C$/$R53A_C$ double mutant accumulated PS I to 30% of wild-type levels while the $K52S_C$/$R53D_C$ and $K52P_C$/$R53D_C$ double mutants resulted in a strong destabilization, and hence little accumulation, of PS I. The in vivo generated $K52S_C$/$R53A_C$ and $K52S_C$/$R53D_C$ mutants in *Ch. reinhardtii* were photosensitive when grown aerobically but could grow photoautotrophically under anaerobic conditions (*43*). It was proposed that solvent accessibility is important for the stability of the iron−sulfur clusters, which are denatured by oxidizing substances such as superoxide (*43*). Our data support a similar mechanism involving oxidative denaturation except that because the loss of electron transfer throughput occurs in the dark, dioxygen is the denaturant rather than superoxide. We further speculate that organisms with mutations on PsaA or PsaB that are unable to grow photoautotrophically may have similarly lost the tight interface with PsaC due to subtle changes in their three-dimensional structure(s) (see ref (*44*)).

The purpose of the extraordinarily tight binding interface between PsaC and the PsaA/PsaB heterodimer in excluding oxygen is also consistent with an analysis of its homologues in homodimeric type I reaction centers of anoxygenic phototrophs. In *Heliobacterium modesticaldum,* PshB is bound to the PshA homodimeric core without the extensive ionic contacts present between PsaC and the PsaA/PsaB heterodimer (*45*). The same is the case for the binding of PscB to the PscA homodimeric core in *Chlorobium tepidum* (*46*), although a PsaD-like subunit (PscD) has been proposed to stabilize PscB on the membrane core (*47*) . These PsaC equivalents are loosely bound and are dissociated from the homodimeric reaction centers at relatively low ionic strengths (*48*, *49*). The critical difference is that unlike plants and cyanobacteria, *Chlorobium* and heliobacteria are strict anaerobes. The PsaC analogues PscB and PshB would not require a tight binding interface with the membrane-bound reaction center core to protect their F_A and F_B clusters from denaturation by photosynthetically generated dioxygen.

It is widely accepted that heterodimeric PS I reaction centers evolved from an ancestral homodimeric type I reaction center (*50*, *51*). The need to protect the F_A and F_B clusters from oxidative denaturation would have occurred at the onset of an oxygen-containing atmosphere, which according to most estimates, occurred ~2.7 billion years ago (*52*, *53*). Our proposal is that the transition to oxygenic photosynthesis involved the tightening of the interface between the membrane-intrinsic

reaction center core proteins and the membrane-extrinsic dicluster ferredoxin to render the latter immobile, thereby protecting F_A and F_B against oxidative degradation. This would have been achieved by the development of an array of charged residues around the F_X and F_A/F_B clusters, thus facilitating the formation of an exceedingly tight-binding interface between PsaC and the PsaA/PsaB subunits. The elaboration of the PsaC subunit also involved the addition of a hydrophobic C-terminal extension to a preexisting bacterial dicluster ferredoxin, which oriented the PsaC protein relative to the newly formed PsaA/PsaB heterodimer and additionally ensured that the [4Fe-4S] clusters were protected against oxidative denaturation. The unintended consequence of the tight binding of PsaC is that an additional protein, an oxygen-insensitive electron carrier, would have been needed to transfer the electron from the acceptor side of PS I to the proteins that require electron reduction. This would have led to the evolution of the oxygen-insensitive [2Fe-2S] ferredoxin, which was one of the very first electron transfer proteins to be discovered in oxygenic photosynthesis.

ACKNOWLEDGMENT

We thank Dr. Ramakrishnan Balasubramanian for his assistance with the site-directed mutagenesis of the *psaC* gene.

REFERENCES

1. Setif, P., Seo, D., and Sakurai, H. (2001) Photoreduction and reoxidation of the three iron-sulfur clusters of reaction centers of green sulfur bacteria. *Biophys. J. 81*, 1208–1219.
2. Setif, P., Fischer, N., Lagoutte, B., Bottin, H., and Rochaix, J. D. (2002) The ferredoxin docking site of Photosystem I. *Biochim. Biophys. Acta 1555*, 204–209.
3. Muller, M. G., Niklas, J., Lubitz, W., and Holzwarth, A. R. (2003) Ultrafast transient absorption studies on Photosystem I reaction centers from *Chlamydomonas reinhardtii*. 1. A new interpretation of the energy trapping and early electron transfer steps in Photosystem I. *Biophys. J. 85*, 3899–3922.
4. Brettel, K. (1997) Electron transfer and arrangement of the redox cofactors in Photosystem I. *Biochim. Biophys. Acta 1318*, 322–373.
5. Parrett, K. G., Mehari, T., Warren, P. G., and Golbeck, J. H. (1989) Purification and properties of the intact P_{700} and F_X-containing Photosystem I core protein. *Biochim. Biophys. Acta 973*, 324–332.
6. Zhao, J., Warren, P. V., Li, N., Bryant, D. A., and Golbeck, J. H. (1990) Reconstitution of electron transport in Photosystem I with PsaC and PsaD proteins expressed in *Escherichia coli*. *FEBS Lett. 276*, 175–180.
7. Li, N., Zhao, J. D., Warren, P. V., Warden, J. T., Bryant, D. A., and Golbeck, J. H. (1991) PsaD is required for the stable binding of PsaC to the Photosystem I core protein of *Synechococcus* sp. PCC 6301. *Biochemistry 30*, 7863–7872.
8. Yu, J., Smart, L. B., Jung, Y. S., Golbeck, J., and McIntosh, L. (1995) Absence of PsaC subunit allows assembly of Photosystem I core but prevents the binding of PsaD and PsaE in *Synechocystis* sp. PCC 6803. *Plant Mol. Biol. 29*, 331–342.
9. Chitnis, V. P., Jung, Y. S., Albee, L., Golbeck, J. H., and Chitnis, P. R. (1996) Mutational analysis of Photosystem I polypeptides: Role of PsaD and the lysyl 106 residue in the reductase activity of Photosystem I. *J. Biol. Chem. 271*, 11772–11780.
10. Zhao, J., Snyder, W. B., Muhlenhoff, U., Rhiel, E., Warren, P. V., Golbeck, J. H., and Bryant, D. A. (1993) Cloning and characterization of the psaE gene of the cyanobacterium *Synechococcus* sp. PCC 7002: Characterization of a psaE mutant and overproduction of the protein in *Escherichia coli*. *Mol. Microbiol. 9*, 183–194.
11. Jordan, P., Fromme, P., Witt, H. T., Klukas, O., Saenger, W., and Krauss, N. (2001) Three dimensional structure of Photosystem I at 2.5 Å resolution. *Nature 411*, 909–917.
12. Vassiliev, I. R., Jung, Y. S., Yang, F., and Golbeck, J. H. (1998) PsaC subunit of Photosystem I is oriented with iron-sulfur cluster F_B as the immediate electron donor to ferredoxin and flavodoxin. *Biophys. J. 74*, 2029–2035.
13. DiazQuintana, A., Leibl, W., Bottin, H., and Sétif, P. (1998) Electron transfer in Photosystem I reaction centers follows a linear pathway in which iron-sulfur cluster F_B is the immediate electron donor to soluble ferredoxin. *Biochemistry 37*, 3429–3439.
14. Antonkine, M. L., Jordan, P., Fromme, P., Krauss, N., Golbeck, J. H., and Stehlik, D. (2003) Assembly of protein subunits within the stromal ridge of Photosystem I. Structural changes between unbound and sequentially PS I-bound polypeptides and correlated changes of the magnetic properties of the terminal iron sulfur clusters. *J. Mol. Biol. 327*, 671–697.
15. Fromme, P., and Grotjohann, I. (2008) Structure of Photosystems I and II. *Results Probl. Cell Differ. 45*, 33–72.
16. Antonkine, M. L., Liu, G., Bentrop, D., Bryant, D. A., Bertini, I., Luchinat, C., Golbeck, J. H., and Stehlik, D. (2002) Solution structure of the unbound, oxidized Photosystem I subunit PsaC, containing [4Fe-4S] clusters F_A and F_B: A conformational change occurs upon binding to Photosystem I. *J. Biol. Inorg. Chem. 7*, 461–472.
17. Zhao, J., Li, R., and Bryant, D. A. (1998) Measurement of Photosystem I activity with photoreduction of recombinant flavodoxin. *Anal. Biochem. 264*, 263–270.
18. Diaz, A., Navarro, F., Hervas, M., Navarro, J. A., Chavez, S., Florencio, F. J., and De la Rosa, M. A. (1994) Cloning and correct expression in *E. coli* of the petJ gene encoding cytochrome c6 from *Synechocystis* 6803. *FEBS Lett. 347*, 173–177.
19. Vassiliev, I. R., Jung, Y. S., Mamedov, M. D., Semenov, A., and Golbeck, J. H. (1997) Near-IR absorbance changes and electrogenic reactions in the microsecond-to-second time domain in Photosystem I. *Biophys. J. 72*, 301–315.
20. Jolley, C. C., Wells, S. A., Hespenheide, B. M., Thorpe, M. F., and Fromme, P. (2006) Docking of Photosystem I subunit C using a constrained geometric simulation. *J. Am. Chem. Soc. 128*, 8803–8812.
21. Jagannathan, B., and Golbeck, J. (2009) Breaking biological symmetry in membrane proteins: The asymmetrical orientation of PsaC on the pseudo-C_2 symmetric Photosystem I core. *Cell. Mol. Life Sci. 66*, 1257–1270.
22. Antonkine, M. L., Maes, E. M., Czernuszewicz, R. S., Breitenstein, C., Bill, E., Falzone, C. J., Balasubramanian, R., Lubner, C., Bryant, D. A., and Golbeck, J. H. (2007) Chemical rescue of a site-modified ligand to a [4Fe-4S] cluster in PsaC, a bacterial-like dicluster ferredoxin bound to Photosystem I. *Biochim. Biophys. Acta 1767*, 712–724.
23. Parrett, K. G., Mehari, T., and Golbeck, J. H. (1990) Resolution and reconstitution of the cyanobacterial Photosystem I complex. *Biochim. Biophys. Acta 1015*, 341–352.
24. Vassiliev, I. R., Antonkine, M. L., and Golbeck, J. H. (2001) Iron-sulfur clusters in type I reaction centers. *Biochim. Biophys. Acta 1507*, 139–160.
25. Moser, C. C., Keske, J. M., Warncke, K., Farid, R. S., and Dutton, P. L. (1992) Nature of biological electron transfer. *Nature 355*, 796–802.
26. Schlodder, E., Falkenberg, K., Gergeleit, M., and Brettel, K. (1998) Temperature dependence of forward and reverse electron transfer from A_1^-, the reduced secondary electron acceptor in Photosystem I. *Biochemistry 37*, 9466–9476.
27. Stephens, P. J., Jollie, D. R., and Warshel, A. (1996) Protein control of redox potentials of iron-sulfur proteins. *Chem. Rev. 96*, 2491–2514.
28. Shinkarev, V. P., Vassiliev, I. R., and Golbeck, J. H. (2000) A kinetic assessment of the sequence of electron transfer from F_X to F_A and further to F_B in Photosystem I: The value of the equilibrium constant between F_X and F_A. *Biophys. J. 78*, 363–372.
29. Shinkarev, V. (2007) Functional modeling of electron transfer in photosynthetic reaction centers. In Photosystem I, The Light-driven Plastocyanin: Ferredoxin Oxidoreductase (Golbeck, J. H., Ed.) pp 611−637, Springer, Dordrecht, The Netherlands.
30. Golbeck, J. H. (2004) Photosynthetic reaction centers: So little time, so much to do. In Biophysics Textbook Online, http://www.biophysics.org/education/golbeck.pdf.
31. Noodleman, L., Norman, J. G.Jr., Osborne, J. H., Aizman, A., and Case, D. A. (1985) Models for ferredoxins: Electronic structures of iron-sulfur clusters with one, two and four iron atoms. *J. Am. Chem. Soc. 107*, 3418–3426.
32. Noodleman, L., Peng, C. Y., Case, D. A., and Mouesca, J. M. (1995) Orbital interactions, electron delocalization and spin coupling in iron-sulfur clusters. *Coord. Chem. Rev. 144*, 199–244
33. Golbeck, J. H. (1999) A comparative analysis of the spin state distribution of *in vivo* and *in vitro* mutants of PsaC. A biochemical argument for the sequence of electron transfer in Photosystem I as $F_X \rightarrow F_A \rightarrow F_B \rightarrow$ ferredoxin/flavodoxin. *Photosynth. Res. 61*, 107–149.
34. Jung, Y. S., Vassiliev, I. R., Yu, J., McIntosh, L., and Golbeck, J. H. (1997) Strains of *Synechocystis* sp. PCC 6803 with altered PsaC. II. EPR and optical spectroscopic properties of F_A and F_B in aspartate, serine, and alanine replacements of cysteines 14 and 51. *J. Biol. Chem. 272*, 8040–8049.
35. Jung, Y. S., Yu, J., Yu, L., Zhao, J., Bryant, D. A., McIntosh, L., and Golbeck, J. H. (1995) *In vivo* site-directed mutations of the cysteine

ligands to F_A and F_B in *Synechocystis* sp. PCC 6803: A comparison with *in vitro* reconstituted Photosystem I complexes. In Photosynthesis: From Light to Biosphere (Mathis, P. A., Ed.) pp 127−130, Kluwer Academic Publishers, Montpellier, France.
36. Jung, Y. S., Vassiliev, I. R., Qiao, F., Yang, F., Bryant, D. A., and Golbeck, J. H. (1996) Modified ligands to F_A and F_B in photosystem I. Proposed chemical rescue of a [4Fe-4S] cluster with an external thiolate in alanine, glycine, and serine mutants of PsaC. *J. Biol. Chem. 271*, 31135–31144.
37. Sticht, H., and Rosch, P. (1998) The structure of iron-sulfur proteins. *Prog. Biophys. Mol. Biol. 70*, 95–136.
38. Bertini, I., Donaire, A., Feinberg, B. A., Luchinat, C., Piccioli, M., and Yuan, H. (1995) Solution structure of the oxidized 2[4Fe-4S] ferredoxin from *Clostridium pasteurianum*. *Eur. J. Biochem. 232*, 192–205.
39. Adman, E. T., Siefker, L. C., and Jensen, L. H. (1976) Structure of *Peptococcus aerogenes* ferredoxin. Refinement at 2 Å resolution. *J. Biol. Chem. 251*, 3801–3806.
40. Harklau, H., Ljones, T., and Skjeldal, L. (2001) Oxygen disruption of the 2[4Fe-4S] clusters in *Clostridium pasteurianum* ferredoxin shown by ^{1}H-NMR. *J. Inorg. Biochem. 85*, 117–122.
41. Adman, E. T., Sieker, L. C., and Jensen, L. H. (1973) The structure of a bacterial ferredoxin. *J. Biol. Chem. 248*, 3987–3996.
42. Golbeck, J. H., Lien, S., and San Pietro, A. (1977) Isolation and characterization of a subchloroplast particle enriched in iron-sulfur protein and P_{700}. *Arch. Biochem. Biophys. 178*, 140–150.
43. Fischer, N., Setif, P., and Rochaix, J. D. (1997) Targeted mutations in the psaC gene of *Chlamydomonas reinhardtii*: Preferential reduction of F_B at low temperature is not accompanied by altered electron flow from Photosystem I to ferredoxin. *Biochemistry 36*, 93–102.
44. Fairclough, W. V., Forsyth, A., Evans, M. C., Rigby, S. E., Purton, S., and Heathcote, P. (2003) Bidirectional electron transfer in Photosystem I: Electron transfer on the PsaA side is not essential for phototrophic growth in *Chlamydomonas*. *Biochim. Biophys. Acta 1606*, 43–55.
45. Heinnickel, M., and Golbeck, J. H. (2007) Heliobacterial photosynthesis. *Photosynth. Res. 92*, 35–53.
46. Hauska, G., Schoedl, T., Remigy, H., and Tsiotis, G. (2001) The reaction center of green sulfur bacteria. *Biochim. Biophys. Acta 1507*, 260–277.
47. Tsukatani, Y., Miyamoto, R., Itoh, S., and Oh-Oka, H. (2004) Function of a PscD subunit in a homodimeric reaction center complex of the photosynthetic green sulfur bacterium *Chlorobium tepidum* studied by insertional gene inactivation. Regulation of zenergy transfer and ferredoxin-mediated $NADP^+$ reduction on the cytoplasmic side. *J. Biol. Chem. 279*, 51122–51130.
48. Heinnickel, M., Shen, G., Agalarov, R., and Golbeck, J. H. (2005) Resolution and reconstitution of a bound Fe-S protein from the photosynthetic reaction center of *Heliobacterium modesticaldum*. *Biochemistry 44*, 9950–9960.
49. Jagannathan, B., and Golbeck, J. H. (2008) Unifying principles in homodimeric type I photosynthetic reaction centers: Properties of PscB and the F_A, F_B and F_X iron-sulfur clusters in green sulfur bacteria. *Biochim. Biophys. Acta 1777*, 1535–1544.
50. Blankenship, R. E. (1992) Origin and early evolution of photosynthesis. *Photosynth. Res. 33*, 91–111.
51. Olson, J. M., and Blankenship, R. E. (2004) Thinking about the evolution of photosynthesis. *Photosynth. Res. 80*, 373–386.
52. Kasting, J. F. (2001) Earth history. The rise of atmospheric oxygen. *Science 293*, 819–820.
53. Olson, J. M. (2006) Photosynthesis in the Archean era. *Photosynth. Res. 88*, 109–117.